IEEE Photonics Journal
An IEEE Photonics Society Publication

Open Access

Duration Switchable High-Energy Passively Mode-Locked Raman Fiber Laser Based on Nonlinear Polarization Evolution

Volume 7, Number 5, October 2015

Jun Liu
Yu Chen
Pinghua Tang
Lili Miao
Chujun Zhao
Shuangchun Wen
Dianyuan Fan

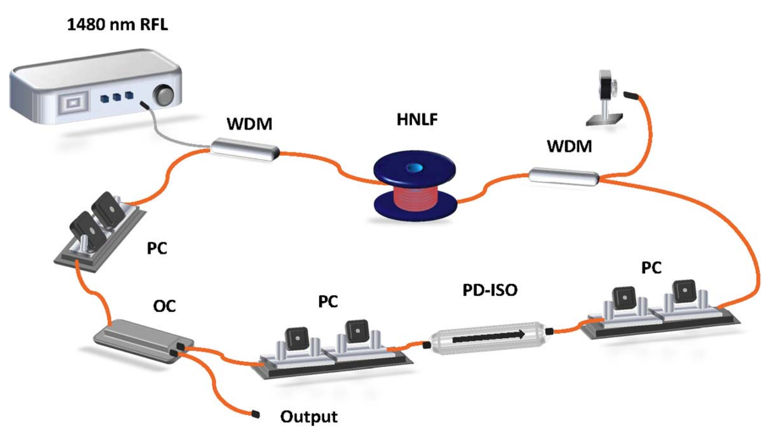

DOI: 10.1109/JPHOT.2015.2477515

Duration Switchable High-Energy Passively Mode-Locked Raman Fiber Laser Based on Nonlinear Polarization Evolution

Jun Liu,[1] Yu Chen,[1] Pinghua Tang,[2] Lili Miao,[2] Chujun Zhao,[1,2] Shuangchun Wen,[2] and Dianyuan Fan[1]

[1]SZU-NUS Collaborative Innovation Center for Optoelectronic Science and Technology, Key Laboratory of Optoelectronic Devices and Systems of Ministry of Education and Guangdong Province, College of Optoelectronic Engineering, Shenzhen University, Shenzhen 518060, China
[2]Key Laboratory for Micro-/Nano-Optoelectronic Devices of Ministry of Education, School of Physics and Electronics, Hunan University, Changsha 410082, China

DOI: 10.1109/JPHOT.2015.2477515

Manuscript received July 12, 2015; revised August 30, 2015; accepted September 4, 2015. Date of publication September 9, 2015; date of current version September 18, 2015. This work was supported in part by the National 973 Program of China under Grant 2012CB315701; by the National Natural Science Foundation of China under Grant 61505124, Grant 61435010, and Grant 61475102; and by the China Postdoctoral Science Foundation under Grant 2015M570721. Corresponding author: C. Zhao (e-mail: chujunzhao@gmail.com).

Abstract: We experimentally demonstrate a stable passively mode-locked Raman fiber laser delivering high-energy pulses that can be switched between the regime of hundreds of nanoseconds and that of picoseconds by the nonlinear polarization rotation technique. Maximum average output power values of 304 and 53 mW are obtained, respectively, for the two typical mode-locking states with the pulse duration of 500 ns and 180 ps at the fundamental repetition rate of 275 kHz. The corresponding single pulse energy is as much as 1.1 μJ and 193 nJ, respectively. To the best of our knowledge, this is the highest pulse energy achieved from mode-locked Raman fiber lasers reported so far.

Index Terms: Raman fiber laser, high energy, mode-locking, nonlinear polarization rotation.

1. Introduction

High-energy wavelength-versatile mode-locked lasers with the pulse duration ranging from femtosecond to the nanosecond order have attracted considerable attention due to their potential applications, including optical communications, remote sensing, and laser micromachining. As we know, appropriate elongation of the laser cavity can simply reduce the pulse repetition rate and thus the per-pulse energy can be scaled up accordingly for a given average output power in mode-locked lasers. So far, numerous long-cavity fiber ring lasers with ultra-high-energy pulses and low repetition rates have been reported based on traditional rare-earth doped ions such as Yb or Er [1], [2]. However, the operating wavelengths were largely restricted to a specific waveband range determined by the gain medium while for some applications the operating wavelength agility is greatly required for the pulses together with their high pulse energy.

Stimulated Raman scattering (SRS), known as a third-order nonlinear effect, can emit at a broad wavelength range that traditional rare-earth-doped fiber lasers cannot cover. This is attributed to the flexible Raman gain that is available at any wavelength across the transparency

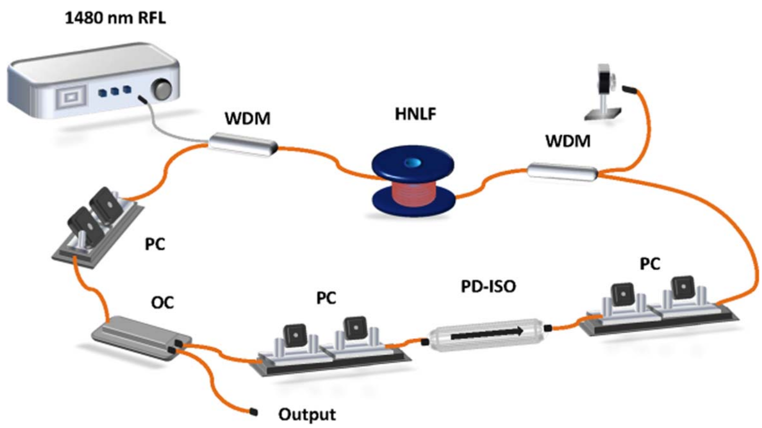

Fig. 1. Experimental schematic of the mode-locked Raman fiber laser based on NPR.

window of silica (300 nm–2200 nm), provided a suitable pump source, is available [3]. To date, continuous-wave (CW) high power Raman fiber lasers and amplifiers based on the SRS effect have been demonstrated at several special laser emissions, such as in the wavelength region of 1.1–1.3 μm [4], [5], 1.4–1.5 μm [6], [7], and 1.6–1.7 μm [8], [9] that cannot be reached by traditional lasers based on rare-earth ion doping. This concept of wavelength versatility can also be applied in ultrashort-pulsed laser sources, such as mode-locked lasers, owing to the broad Raman gain bandwidth. Furthermore, mode-locked Raman fiber lasers, characterized by their relatively long cavities, can also scale up the single pulse energy in addition to their wavelength agility.

Recently, passively mode-locked Raman fiber lasers have been demonstrated using several mode-locking techniques, such as nonlinear polarization rotation (NPR) [10], nonlinear amplifying loop mirror (NALM) [11] or other real saturable absorbers [12]–[14]. However, the per-pulse energies of the mode-locked Raman fiber lasers demonstrated have been limited to a low level of several nanojoules. In addition, mode-locked pulse trains from some typical mode-locked Raman fiber lasers have exhibited an uneven pulse pattern with a low-frequency envelope under different pumping conditions [10] or shown a significant autocorrelation pedestal suffering from long-term temporal instabilities and the pulse-to-pulse energy fluctuations [11], [12]. These shortcomings will therefore further limit their applicability.

In this paper, we experimentally demonstrate high energy operation of a mode-locked Raman fiber laser based on the NPR technique. The long cavity length but with small net dispersion in the mode-locked Raman fiber laser allowed the single pulse energy to be scaled up to 1.1 μJ without pulse breaking for the typical nanosecond mode-locking state at the fundamental frequency of 275 kHz. The corresponding single pulse duration was 500 ns. To the best of our knowledge, this is the highest single pulse energy achieved so far from mode-locked Raman fiber lasers. By adjusting cavity conditions, another stable fundamental mode-locking operation was realized with a maximum average output power of 53 mW and single pulse duration of 180 ps, corresponding to a per-pulse energy of 193 nJ. Ultimately, other typical mode-locking regimes including multi-pulse operation were also observed in our experiment. Their mode-locking behaviors and characteristics have been compared and analyzed.

2. Experimental Setup

The experimental schematic diagram of the mode-locked Raman fiber laser is depicted in Fig. 1. The all-fiber ring laser cavity consists of a piece of 710 m single-mode highly nonlinear fiber (HNLF) (OFS, Furukawa) as the Raman gain medium, two 1480/1580 nm wavelength-division-multiplexed (WDM) couplers, three sets of polarization controllers (PCs), a polarization-dependent isolator (PD-ISO), and a fused 30% output coupler (OC). A 1480 nm commercial high-power

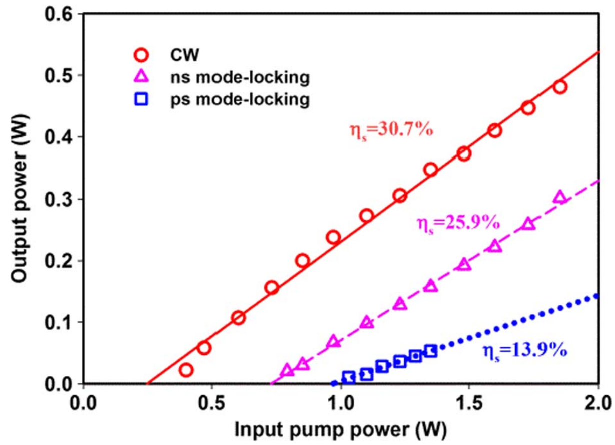

Fig. 2. Average output power versus pump power in the CW and typical mode-locking operation regimes including the nanosecond mode-locking and picosecond mode-locking states.

single-mode Raman laser with a maximum output power of up to 10 W (KEOPSYS) was used as the pump source, and from this, the laser output was directly backward coupled into the Raman fiber through the 1480/1580 nm WDM coupler. A second WDM coupler was employed to extract the un-depleted pump power out of the cavity to prevent damaging the passive cavity components. The PD-ISO and three PCs, together of which operate as an artificial saturable absorber, are responsible for the stable mode-locking of the Raman fiber laser.

The Raman fiber of HNLF was designed to have a zero dispersion wavelength at 1550 nm with a dispersion slope as low as 0.017 ps/(nm^2•km), a nonlinear coefficient of 11.3 /(W•km) and loss of 1.06 dB/km at this wavelength. The rest fibers in the cavity are the standard single-mode telecom fibers (SMFs) with group velocity dispersion (GVD) of 17 ps/(nm•km) at 1550 nm. The total cavity length is about 730 m, resulting in a fundamental repetition rate of ˜275 kHz, a total loss of 0.8 dB, and a slightly negative net cavity dispersion of –0.45 ps^2 at the first order Stokes wavelength range. The output spectrum and temporal profile from this laser was simultaneously monitored by an optical spectrum analyzer (Ando, AQ-6317B) and a real-time oscilloscope with a bandwidth of 4 GHz (Agilent Technol., DSO9404A), together with a 12 GHz photoelectric detector (rise time ~18 ps), respectively. A RF-spectrum analyzer (Agilent, N9322C) was also used to analyze the relative pulse characteristics.

3. Results and Discussions

The lasing characteristics of the Raman fiber laser in the CW regime were evaluated first. Once the laser was first started without carefully adjusting the PCs, it presented a CW operation regime with large dependence of output power and lasing wavelength on the intracavity polarization state. In this situation, passive mode-locking, based on the pulse shortening effect resulting from an artificial intensity filter formed by NPR, was not initiated. Under the CW operating condition, we maximized the output power through the proper alignment of the three PCs. The output power as a function of the input pump power is shown in Fig. 2. A maximum output power of 480 mW was achieved at 1594.6 nm with a broadened FWHM bandwidth of 22 nm due to the largely accumulated nonlinearity, corresponding to a slope efficiency of 30.7% with respect to the pump power. The threshold pump power was measured to be around 400 mW, from which we estimate the Raman gain coefficient of the HNLF to be ~2 W^{-1}km^{-1}. Slight adjustment of the intracavity PCs can deeply modify the center laser wavelength ranging from 1570 to 1595 nm and spanning several tens of nanometers due to the polarization dependence in the laser cavity. Higher order Stokes laser emissions were not observed over the whole tuning and pump power increasing process.

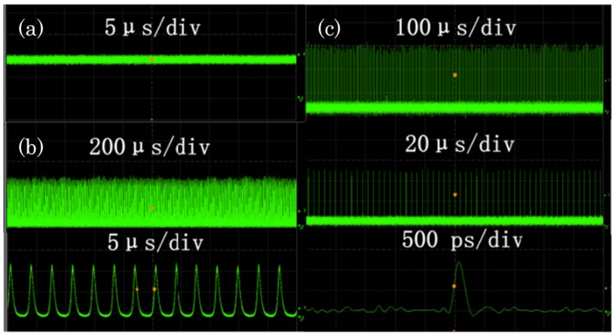

Fig. 3. Temporal profiles of the CW and two stable mode-locking regimes. (a) CW operation regime, (b) nanosecond mode-locking regime, and (c) picosecond mode-locking regime.

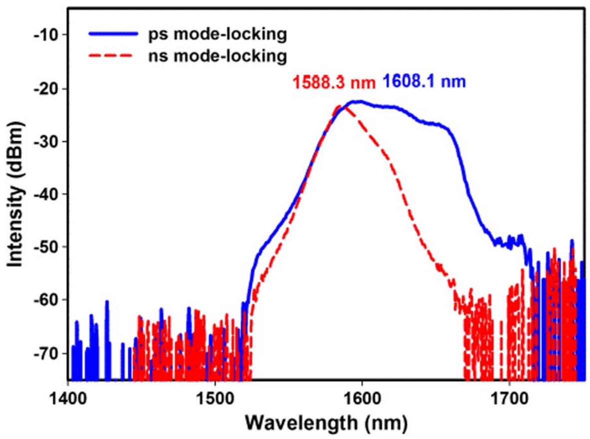

Fig. 4. Measured output spectra of the two stable mode-locking operation regimes.

3.1. Nanosecond Mode-Locking Regime

Since birefringence- and Kerr-induced changes in polarization states can dramatically affect the temporal dynamics from Raman fiber lasers [15], [16], we adjusted the orientations of the intracavity PCs at a high enough pump power, and a highly stable mode-locked pulse train in the regime of several hundreds of nanoseconds could be easily achieved at the fundamental repetition rate of 275 kHz. The mode-locked pulse train recorded at different time scales with a typical pulse duration of 500 ns is shown in Fig. 3(b), while Fig. 3(a) gives the temporal profile in the regime of CW operation for comparison. The average output power as a function of input pump power in this mode-locking regime is also shown in Fig. 2. It is worth noting that the average output power increased almost linearly with the pump power without showing any signs of saturation. A maximum average output power of 304 mW was obtained at the pump power of 1.85 W, corresponding to a single pulse energy of up to 1.1 μJ. The corresponding output spectrum centered at 1588.3 nm gradually increased to as much as 20 nm (3 dB bandwidth) due to the nonlinear spectral broadening through self-phase modulation (SPM), as shown in Fig. 4. The stable nanosecond mode-locking state still remained with pulse duration slightly changed and no pulse breaking during the whole pump increasing process. We did not attempt to further scale up the output power and pulse energy in case of damaging the in-fiber optical components. It can also be seen in Fig. 2 that the mode-locking operation regime exhibits a higher pump threshold of ~800 mW and lower slope efficiency of 25.9%, which is attributed to a significant cavity loss in a more demanding condition satisfying the Raman mode-locking. The RF spectrum of the laser output is shown in Fig. 5. The center frequency corresponds to the fundamental pulse repetition

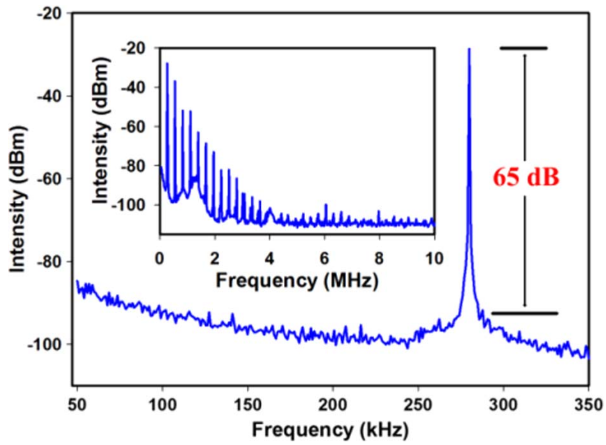

Fig. 5. RF spectrum of the nanosecond mode-locked pulses.

rate of 275 kHz with signal-to-noise ratio (SNR) of about 65 dB, indicating good mode-locking stability and low pulse timing jitter.

3.2. Picosecond Mode-Locking Regime

After finely and carefully adjusting the intracavity PCs to vary the cavity birefringence, another mode-locking state in the regime of several hundreds of picoseconds was obtained near the pump threshold. The corresponding pulse trains with different time scales are shown in Fig. 3(c). Different from the nanosecond mode-locking regime, the mode-locked pulses in this regime were largely shortened. The average output power of the stable mode-locked pulse train at the fundamental repetition rate can be scaled up to 53 mW with the pulse duration of 180 ps by simply increasing the pump power, as shown in Fig. 2. The corresponding single pulse energy was as much as 193 nJ. The output spectrum is shown in Fig. 4, with the center wavelength of 1608.1 nm and a 3 dB bandwidth of 54 nm, which is much broader than the spectrum in the nanosecond mode-locking regime. The SNR of the fundamental frequency was measured to be more than 50 dB. A further increase of the pump power will render the system unstable, and ultimately evolving into the multi-pulse operation.

When the pump power was elevated to more than 1.35 W, the laser also exhibits other typical pulsed regimes with multi-pulses coexisting in the cavity after finely adjusting the PCs, as shown in Fig. 6. Fig. 6(a) shows a stable mode-locked pulse train but located on an unordered smooth pedestal that does not persist for long time. The oscilloscope traces of the stable multi-pulse mode-locking regimes recorded at a constant input pump power are shown in Fig. 6(b) and (c), illustrating the situations of two-pulse and multi-pulse bunch coexisting in the cavity, respectively. The multi-pulse operation regime was also attributed to the peak power clamping and soliton quantization effect [17].

3.3. Discussions

The most striking characteristic in our experiment is the two stable high energy mode-locking states obtained with switchable pulse durations by adjusting the cavity conditions. This can be attributed to the pulse narrowing differences imposed by NPR for different orientations of the intracavity PCs in the two regimes. Typically, the polarization state in a Raman fiber laser can have a crucial importance to the dynamical behavior of the laser output. Depending on different polarization conditions resulting from the PC alignment in the cavity, the pulse dynamics toward instabilities may take various forms with different time profiles and periods. Similarly, in the ring Raman fiber laser of our experiment, different polarization orientations combined with the NPR mode-locking technique can result in different pulse narrowing processes, shaping the resultant

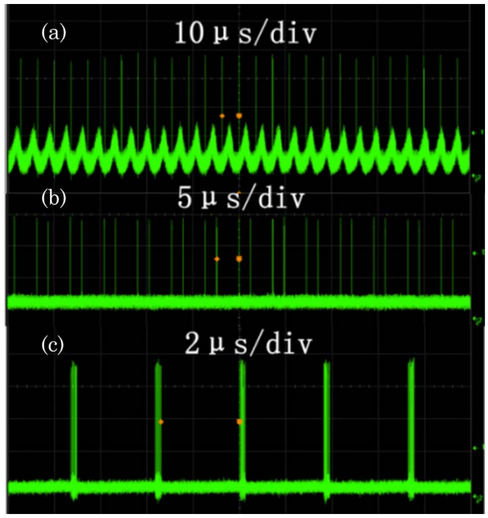

Fig. 6. Temporal pulse trains of typical unordered (a) or stable multi-pulse mode-locking regimes (b) and (c).

mode-locking regimes with different order of pulse durations. A much broader spectrum was achieved in the regime of picosecond mode-locking than the nanosecond operation regime, which is attributed to the much larger nonlinearity accumulated in the former situation resulting from the higher intracavity peak power. In addition, the small dispersion differences across the output spectral component for the mode-locking state of hundreds of nanoseconds allows the pulses to be scaled up to a high level of energy without pulse breaking, despite a largely broadened spectrum due to the large nonlinearity.

The main challenge to achieve stable mode-locking based on NPR in Raman fiber lasers was to find the transition from CW operation to the pulsed regime, and then stabilize the mode-locked laser pulses through the slight modifications of the PC orientations. It is worth noting that the mode-locking operation with simultaneous Raman conversion arises from the interactive coupling between the NPR and the operating wavelength of Stokes laser. On the other hand, the counteracting influence of the stimulated Raman conversion to the pulse stabilization during the mode-locking buildup process should be optimized to reach maximum lasing efficiency. In addition, the cavity dispersion and nonlinearity, such as the optical Kerr effect, may deeply influence the mode-locking dynamics including the pulse shape and duration. These relationships and mechanism of Raman mode-locking based on NPR will be further investigated in our later experiments.

4. Conclusion

In conclusion, we have experimentally demonstrated stable and high energy operation of a passively mode-locked Raman fiber laser based on the NPR technique. Two typical switchable Raman mode-locking regimes, with different order of magnitude of pulse duration of several hundreds of nanoseconds or picoseconds, have been achieved at the first order Stokes wavelength by finely adjusting the cavity conditions. For the nanosecond mode-locking regime, a maximum average output power of 304 mW at the fundamental repetition rate of 275 kHz is obtained, corresponding to a single pulse packet energy of up to 1.1 μJ with the duration of 500 ns. Another stable picosecond mode-locking state corresponds to a maximum single pulse energy of 193 nJ with a pulse duration of 180 ps. To the best of our knowledge, this is the highest pulse energy reported to date from mode-locked Raman fiber lasers. Mechanism of Raman mode-locking based on NPR and other real saturable absorbers will be further explored in our later research.

References

[1] S. Kobtsev, S. Kukarin, and Y. Fedotov, "Ultra-low repetition rate mode-locked fiber laser with high-energy pulses," *Opt. Exp.*, vol. 16, no. 26, pp. 21936–21941, Dec. 2008.

[2] X. Li *et al.*, "Long-cavity passively mode-locked fiber ring laser with high-energy rectangular-shape pulses in anomalous dispersion regime," *Opt. Lett.*, vol. 35, no. 19, pp. 3249–3251, Oct. 2010.

[3] E. P. Ippen, C. K. N. Patel, and R. H. Stolen, "*Broadband Tunable Raman-Effect Devices in Optical Fibers*," U.S. Patent 3705992, Dec. 12, 1972.

[4] Y. Feng, L. R. Taylor, and D. B. Calia, "150 W highly-efficient Raman fiber laser," *Opt. Exp.*, vol. 17, no. 26, pp. 23678–23683, Dec. 2009.

[5] C. A. Codemard, J. Ji, J. K. Sahu, and J. Nilsson, "100 W CW cladding-pumped Raman fiber laser at 1120 nm," in *Proc. SPIE*, 2010, vol. 7580, Art ID. 75801N.

[6] J. W. Nicholson *et al.*, "Raman fiber laser with 81 W output power at 1480 nm," *Opt. Lett.*, vol. 35, no. 18, pp. 3069–3071, Sep. 2010.

[7] V. R. Supradeepa and J. W. Nicholson, "Power scaling of high-efficiency 1.5 μm cascaded Raman fiber lasers," *Opt. Lett.*, vol. 38, no. 14, pp. 2538–2541, Jul. 2013.

[8] C. A. Codemard *et al.*, "High-power continuous-wave cladding-pumped Raman fiber laser," *Opt. Lett.*, vol. 31, no. 15, pp. 2290–2292, Aug. 2006.

[9] J. Liu *et al.*, "High-power and highly efficient operation of wavelength-tunable Raman fiber lasers based on volume Bragg gratings," *Opt. Exp.*, vol. 22, no. 6, pp. 6605–6612, Mar. 2014.

[10] A. Chamorovskiy *et al.*, "1.38-μm mode-locked Raman fiber laser pumped by semiconductor disk laser," *Opt. Exp.*, vol. 18, no. 23, pp. 23872–23877, Nov. 2010.

[11] D. A. Chestnut and J. R. Taylor, "Wavelength-versatile subpicosecond pulsed lasers using Raman gain in figure-of eight fiber geometries," *Opt. Lett.*, vol. 30, no. 22, pp. 2982–2984, Nov. 2005.

[12] C. E. S. Castellani *et al.*, "Ultrafast Raman laser mode-locked by nanotubes," *Opt. Lett.*, vol. 36, no. 20, pp. 3996–3998, Oct. 2011.

[13] C. E. S. Castellani *et al.*, "Harmonic and single pulse operation of a Raman laser using graphene," *Laser Phy. Lett.*, vol. 9, no. 3, pp. 223–228, Mar. 2012.

[14] L. Zhang *et al.*, "Linearly polarized 1180-nm Raman fiber laser mode locked by graphene," *IEEE Photon. J.*, vol. 4, no. 5, pp. 1809–1815, Oct. 2012.

[15] A. Doutté, P. Suret, and S. Randoux, "Influence of light polarization on dynamics of continuous-wave-pumped Raman fiber lasers," *Opt. Lett.*, vol. 28, no. 24, pp. 2464–2466, Dec. 2003.

[16] P. Suret, A. Doutté, and S. Randoux, "Influence of light polarization on dynamics of all-fiber Raman lasers: Theoretical analysis," *Opt. Lett.*, vol. 29, no. 18, pp. 2166–2168, Sep. 2004.

[17] A. B. Grudinin, D. J. Richardson, and D. N. Payne, "Energy quantization in figure eight fibre laser," *Electron. Lett.*, vol. 28, no. 1, pp. 67–68, Jan. 1992.